

## Preparation of Highly Visible-Light Photocatalytic Active N-Doped TiO<sub>2</sub> Microcuboids

Kang Zhao\*, Zhiming Wu, Rong Tang, and Yadong Jiang

State Key Laboratory of Electronic Thin Films and Integrated Devices, School of Optoelectronic Information,  
University of Electronic Science and Technology of China (UESTC), Chengdu 610054, P.R. China

\*E-mail: 30300698@qq.com

(Received April 3, 2013; Accepted June 26, 2013)

**ABSTRACT.** N-doped TiO<sub>2</sub> microcuboids were successfully prepared by a simple one-pot hydrothermal method. The samples were characterized by X-ray diffraction, scanning electron microscopy, diffuse reflectance spectroscopy, and X-ray photoelectron spectroscopy. It was found that the N-doped TiO<sub>2</sub> microcuboids enhanced absorption in the visible light region, and exhibited higher activity for photocatalytic degradation of model dyes. Based on the experimental results, a visible light induced photocatalytic mechanism was proposed for N-doped anatase TiO<sub>2</sub> microcuboids.

**Key words:** Nitrogen-doping, TiO<sub>2</sub> microcuboid, Visible photocatalyst, Mechanism

### INTRODUCTION

Titanium dioxide (TiO<sub>2</sub>) is the most widely used photocatalytic material since it exhibits non-toxic nature, high efficiency, chemical inertness, relatively low cost, and photostability.<sup>1–4</sup> However, the main drawback is that TiO<sub>2</sub> photocatalysts can only be excited by ultraviolet (UV) light due to their wide band gap. Therefore, many studies have been devoted to the efficiency improvement of TiO<sub>2</sub> under visible light illumination.<sup>5–7</sup>

Over the past twenty years, there has been extensive research into extending the absorption profile of TiO<sub>2</sub> into the visible region by doping with main group elements, in particular with nitrogen. Nitrogen doping is one of the simplest synthetic methods to engineer a visible photocatalyst, and it can narrow the band gap of TiO<sub>2</sub> to 2.6 eV, which consequently gives rise to visible light-driven photocatalytic activity.<sup>8</sup> Since then, N-doped TiO<sub>2</sub> have been prepared by various methods, including sol-gel method,<sup>9</sup> chemical vapor deposition method,<sup>10</sup> hydrothermal method<sup>11</sup> and calcination in ammonia gas.<sup>12</sup> Among them, the hydrothermal route is an ideal technique for synthesizing N-doped TiO<sub>2</sub> nanomaterials with high purity, narrow particle size distribution, controlled morphology and high crystallinity.<sup>13</sup> For example, Zhao<sup>14</sup> and his coworkers prepared N-doped TiO<sub>2</sub> hollow microspheres by a one-step hydrothermal method, and the prepared TiO<sub>2</sub> microspheres showed excellent photocatalytic activities in degrading dyes under visible light irradiation. Liu et al.<sup>15</sup> prepared N-doped TiO<sub>2</sub> nanorods by a simple one-pot sol-

voethermal method using hydrazine hydrate and TiO<sub>2</sub> colloids as the starting materials, and the sample showed high catalytic activity of decomposing methyl orange and 4-chlorophenol under UV and visible light illumination. Despite that several studies have succeeded in the preparation of N-doped TiO<sub>2</sub> nanoparticles with various morphologies, no report, so far, synthesized the N-doped TiO<sub>2</sub> microcuboids with high visible light photocatalytic activity.

In this article, we report a facile way to obtain N-doped TiO<sub>2</sub> microcuboids with high photocatalytic property under UV and visible light irradiation. It was proven that the prepared N-doped TiO<sub>2</sub> microcuboids significantly enhanced the photo absorption abilities and photocatalytic activities as compared to those of TiO<sub>2</sub> samples under the same conditions.

### EXPERIMENTAL DETAILS

All reagents were analytical grade and used without further purification. In a typical procedure, 2.37 g titanium n-butoxide was dissolved into 15 mL of ethanol. 0.05 g sodium dodecyl sulfate (SDS) and 2 mL of ammonia were added into 5 ml of deionized water and stirring continued for 30 min. After sufficient mixing, the mixed solution was added drop wise into the titanium n-butoxide solution with constant stirring. Next, the autoclave was heated at 160 °C for 12 h and allowed to cool down naturally. The product was centrifuged, washed several times with distilled water and ethanol, and dried at 60 °C for 6 h. At last, the sample was then annealed at 450 °C for 3 h in air to

prepare the final N-doped TiO<sub>2</sub> microcuboids. For comparison, the TiO<sub>2</sub> samples were prepared using the same method.

The phase of the as-prepared products was determined by a Rigaku D/Max 2400 X-ray diffractometer (XRD) equipped with graphite monochromatized CuK $\alpha$  radiation. The morphology of the as-synthesized products was observed directly by a JEOL JSM-5600LV scanning electron microscope (SEM) equipped with energy-dispersive X-ray spectroscopy (EDS). The UV-vis diffuse reflectance spectra (DRS) of the samples over a range of 200–800 nm were collected on a UV-2450 instrument.

The evaluation of photocatalytic activity of the prepared samples for the photocatalytic decomposition of RhB aqueous solution under 300 W mercury lamp as a UV source or 300 W Xe lamp served as a visible-light source with an ultraviolet cutoff filter, which allowed the transmission of visible-light with a wavelength longer than 420 nm ( $\lambda > 420$  nm). 50 mg photocatalyst was dispersed in a 50 mL aqueous solution of  $1.0 \times 10^{-5}$  M RhB. Before photodegradation, adsorption equilibrium of the dye on catalyst surface was established by mechanical stirring for 30 min. After solar irradiation for some time (30 min), the reaction solution was filtrated to remove the suspended particulates. Then, the concentration of RhB in solution was analyzed with an UV-visible spectrophotometer (UV-2550, Shimadzu, Japan).

## RESULTS AND DISCUSSION

The typical powder XRD patterns of TiO<sub>2</sub> sample and N-doped TiO<sub>2</sub> microcuboids are shown in Fig. 1. The crystal structures of the N-doped TiO<sub>2</sub> powders represent the anatase phases (JCPDS, card no: 21-1272), which are similar to pure TiO<sub>2</sub> sample.

Fig. 2 shows typical SEM images of the N-doped TiO<sub>2</sub> microcuboids fabricated by a one-pot hydrothermal method. As shown in Fig. 2a, the overall morphology of the sam-

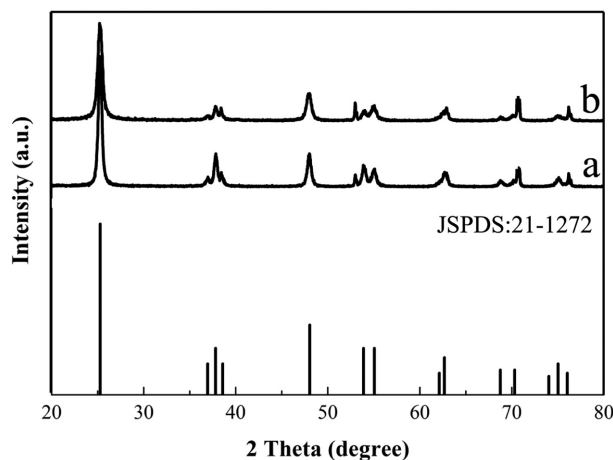


**Figure 1.** XRD patterns of TiO<sub>2</sub> samples (a) and N-doped TiO<sub>2</sub> microcuboids (b).

ple indicates that there exists a great deal of uniform cuboid-like microstructures in high yield. The microcuboids are in the length of about 400 nm, in the width of about 300 nm and in the height of about 250 nm. The corresponding EDS of N-doped TiO<sub>2</sub> microcuboids also demonstrates the presence of Ti, O and N, and the atomic ratio of the N is about 16%.

Fig. 3 shows the corresponding UV-vis diffuse reflectance spectra of pure TiO<sub>2</sub> samples and N-doped TiO<sub>2</sub> microcuboids. The absorption edge of pure TiO<sub>2</sub> samples is observed at about 380 nm, corresponding to the band-gap energy of 3.2 eV. After the N doping in the TiO<sub>2</sub> samples, the absorption spectrum shows that the absorption edge is shifted significantly toward the visible region with a band edge of 535 nm ( $E_g = 2.3$  eV) (Fig. 3b). The remarkable absorbance for visible light is attributed to the formation of the O-Ti-N linkage, leading to the narrowing of the energy band gap. This phenomenon can also be explained in terms of the formation of an intra-band gap located above the valence band, due to substitution of oxide centers by nitride centers and/or to the interstitial

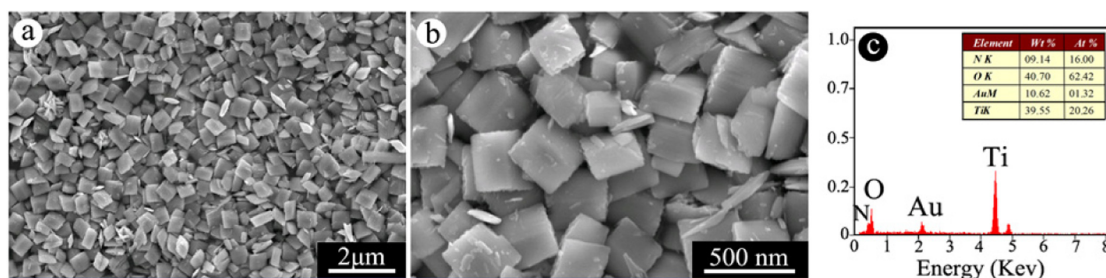


**Figure 2.** SEM images (a, b) and EDS (c) of N-doped TiO<sub>2</sub> microcuboids.

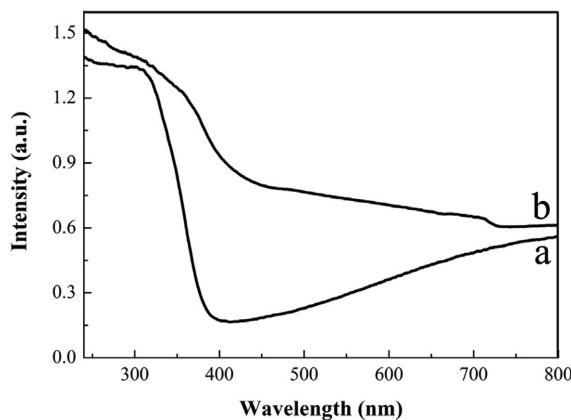


**Figure 3.** UV-vis spectra of TiO<sub>2</sub> samples (a) and N-doped TiO<sub>2</sub> microcuboids (b).

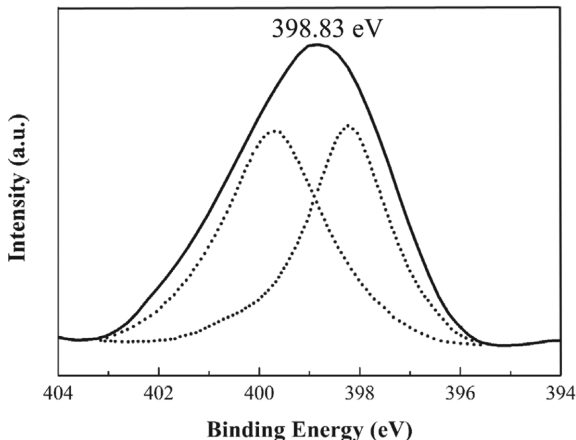


**Figure 4.** N1s XPS patterns spectrum of N-doped TiO<sub>2</sub> microcuboids.

introduction of nitride into the oxide lattice.<sup>16</sup>

Fig. 4 shows the N1s X-ray photoelectron spectroscopy spectrum of the N-doped TiO<sub>2</sub> microcuboids prepared by hydrothermal process. In general, the peak of N1s from the XPS spectrum is mostly found in the range of 396–404 eV. The N1s peak at 399.63 eV can be attributed to the nitrogen in the form of a Ti–N–O linkage, and the low bonding energy component located at 398.23 eV is generally known as the N atom replacing the oxygen atoms in the TiO<sub>2</sub> crystal lattice to form an N–Ti–N bond. The relative atomic concentrations of N in the TiO<sub>2</sub> sample is found to be 4.8 at.% based on the XPS data.

The photocatalytic activity of the TiO<sub>2</sub> samples and N-doped TiO<sub>2</sub> microcuboids was evaluated by measuring the rate of degradation of RhB under UV and visible light irradiation. Fig. 5(a) shows the degradation of RhB under UV irradiation for the two kinds of samples. After 150 min of UV irradiation, 87% of RhB is decomposed by TiO<sub>2</sub> sam-

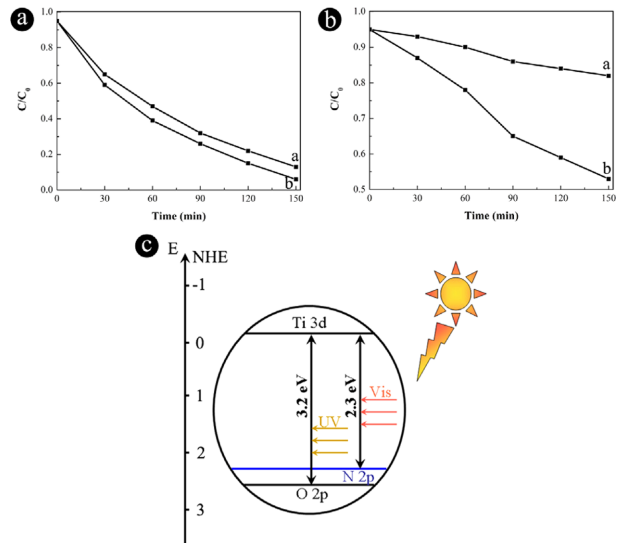


**Figure 5.** The photocatalytic degradation of RhB over TiO<sub>2</sub> samples and N-doped TiO<sub>2</sub> microcuboids under UV (a) and visible light (b) irradiation. A schematic illustration of electron migration in N-doped TiO<sub>2</sub> microcuboids under UV and visible light irradiation (c).

ples, whereas 94% of RhB is decomposed by N-doped TiO<sub>2</sub> microcuboids. It indicates that N-doped TiO<sub>2</sub> microcuboids exhibits superior photocatalytic capability in degrading RhB dye under the UV irradiation, and the photocatalytic enhancement is mainly attributed to the effective separation of the photogenerated electron-holes pairs. Under UV light activation, the electrons of TiO<sub>2</sub> are excited to the conduction band, the valence holes transferred from the valence band of TiO<sub>2</sub> (O2p) to that of TiO<sub>2</sub> (N2p). Thus, electron-hole pairs are effectively separated, which leads to the high photocatalytic activity of N-doped TiO<sub>2</sub> microcuboids. However, under visible light activation, the 47% of RhB removal is obtained after 150 min, while only 18% of the RhB removal is obtained in the photocatalytic process with the same illumination time. It is therefore concluded that N-doping is very important to improve the visible light photocatalytic performance. It is speculated that the main reason is the narrowing of the band gap caused by the mixing of the N2p and O2p states, which resulted in high visible light photocatalytic activity.

## CONCLUSION

In conclusion, N-doped TiO<sub>2</sub> microcuboids were successfully fabricated by a facile one-pot hydrothermal method. The structure, optical and photocatalytic properties of N-doped TiO<sub>2</sub> microcuboids were discussed in

detail, and the novel N-doped TiO<sub>2</sub> microstructures greatly enhanced the visible light response and photocatalytic degradation of RhB. The enhanced photocatalytic properties can be attributed to the extended absorption in the visible light region and the effective separation of photogenerated carriers resulting from N doping in the TiO<sub>2</sub> crystals. This new type of photocatalyst that can harness both UV and visible light presents a promising candidate for applications in photocatalysis.

**Acknowledgments.** This work was financially supported by the National Natural Science Foundation of China (No. 61235006). And the publication cost of this paper was supported by the Korean Chemical Society.

## REFERENCES

1. Yao, F.; Sun, Y.; Tan, C. L.; Wei, S.; Zhang, X. J.; Hu, X. Y.; Fan, J. *J. Korean Phys. Soc.* **2011**, *55*, 932.
2. Chen, W. G.; Yuan, P. F.; Zhang, S.; Sun, Q.; Liang, E.; Jia, Y. *Physica B* **2012**, *407*, 1038.
3. Ebrahimi, R.; Tarhandeh, G.; Rafiey, S.; Narjabadi, M.; Khani, H. *J. Korean Phys. Soc.* **2011**, *56*, 92.
4. Zhao, H. M.; Wu, M. M.; Wang, Q.; Jena, P. *Physica B* **2011**, *406*, 4322.
5. Yan, X. M.; Kang, J. L.; Gao, L.; Xiong, L.; Mei, P. *Appl. Surf. Sci.* **2013**, *265*, 778.
6. Nakajima, T.; Lee, C. Y.; Yang, Y.; Schmuki, P. *J. Mater. Chem. A* **2013**, *1*, 1860.
7. Chen, K. S.; Feng, X. R.; Hu, R.; Li, Y. B.; Xie, K.; Li, Y.; Gu, H. S. *J. Alloys Compd.* **2013**, *554*, 72.
8. Liu, B. K.; Wang, D. J.; Zhang, Y.; Fan, H. M.; Lin, Y. H.; Jiang, T. F.; Xie, T. F. *Dalton Trans.* **2013**, *42*, 2232.
9. Dunnill, C. W.; Ansari, Z.; Kazas, A.; Perni, S.; Morgan, D. J.; Wilson, M.; Parkin, I. P. *J. Mater. Chem.* **2011**, *21*, 11854.
10. Ku, Y.; Chen, W. J.; Hou, W. M. *Sustain. Environ. Res.* **2013**, *23*, 15.
11. Wang, D. H.; Jia, L.; Wu, X. L.; Lu, L. Q.; Xu, A. W. *Nanoscale* **2012**, *4*, 576.
12. Wu, M. C.; Liao, H. C.; Cho, Y. C.; Tóth, G.; Chen, Y. F.; Su, W. F.; Kordás, K. *J. Mater. Chem. A* **2013**, *1*, 5715.
13. Yang, G. D.; Jiang, Z.; Shi, H. H.; Xiao, T. C.; Yan, Z. F. *J. Mater. Chem.* **2010**, *20*, 5301.
14. Pan, J. H.; Han, G.; Zhou, R.; Zhao, X. S. *Chem. Commun.* **2011**, *47*, 6942.
15. Gai, L. G.; Duan, X. Q.; Jiang, H. H.; Mei, Q. H.; Zhou, G. W.; Tian, Y.; Liu, H. *Cryst. Eng. Commun.* **2012**, *14*, 7662.
16. Li, M.; Zhang, J. Y.; Zhang, Y. *Catal. Commun.* **2012**, *29*, 175.